Available online at www.sciencedirect.com
ScienceDirect
Surface Science 601 (2007) 1231–1238
SURFACE SCIENCE
www.elsevier.com/locate/susc

Adsorbed molecular shuttlecocks: An NIXSW study of Sn phthalocyanine on Ag(1 1 1) using Auger electron detection

R.A.J. Woolley [a,b,*], C.P. Martin [a], G. Miller [b], V.R. Dhanak [b], P.J. Moriarty [a]

[a] *Nanoscience Group, School of Physics and Astronomy, University of Nottingham, Nottingham NG7 2RD, United Kingdom*[1]
[b] *Daresbury Laboratory, Warrington, Cheshire WA4 4AD, UK*

Received 5 September 2006; accepted for publication 12 December 2006
Available online 19 December 2006

Abstract

Normal incidence X-ray standing wave (NIXSW) spectroscopy has been used to determine the orientation of Sn phthalocyanine (SnPc) molecules in a highly ordered, but incommensurate, monolayer on the Ag(1 1 1) surface. Our sample preparation procedure differs from that used in previous work on this system [C. Stadler, S. Hansen, F. Pollinger, C. Kumpf, E. Umbach, T.-L. Lee, J. Zegenhagen, Phys. Rev. B 74 (2006) 035404] and leads to a different unit cell with basis vector lengths of ~15.0 Å and 15.3 Å ($\gamma = 98°$) which is oriented at an angle of ~5° to the underlying Ag(1 1 1) lattice. Structural parameters extracted from Sn MNN NIXSW spectra indicate that SnPc, a buckled, 'shuttlecock' phthalocyanine, adsorbs in a Sn-down geometry with the Sn atom approximately 2.3 Å above the Ag(1 1 1) surface plane. Despite the incommensurate nature of the overlayer, we find a surprisingly high coherent fraction for standing wave data taken for the $(\bar{1}\,1\,1)$ reflection and argue that this arises from the small domain size of the superstructure.

Keywords: X-ray standing wave; Low energy electron diffraction (LEED); Phthalocyanine; SnPc; Ag(1 1 1); Photoemission; Binding site; Geometry

1. Introduction

The desire for increased computational power at an ever-reducing physical size per gigaflop is pushing state-of-the-art nanoscale science and technology into the domain of molecular electronics. Organic molecules lend themselves well to the requirements of building electronic circuits not only in terms of their ability to form novel self-assembled structures [1] but also because individual molecules can be used as discrete circuit elements (switches, wires, etc.) [2].

One set of molecules of particular importance in molecular electronics is the phthalocyanine family [3]. Metal phthalocyanines (MePc) are generally planar organic molecules comprising of a central metal atom surrounded by a porphyrin-like unit that in turn is surrounded by four aromatic rings (see inset to Fig. 1). Phthalocyanines are structurally similar to important biomolecules such as haemoglobin and chlorophyll and are commonly used in industry for pigmentation. They have been the focus of intense interest due to their electrical and (non-linear) optical properties. Selection of the central metal atom allows the molecular properties to be tuned *without the addition of functional groups*. For example, by increasing the size of the metal atom the molecule distorts and becomes aplanar [4], as in the case of SnPc which appears shuttlecock shaped with the Sn out of the molecular plane.

Fundamental understanding of molecule–molecule and molecule–surface interactions is important when attempting to determine the charge transport characteristics of metal phthalocyanines. For instance, the adsorption of CuPc on a rough substrate results in the molecular axis aligning perpendicular to the surface. If, however, the molecule is

* Corresponding author. Address: Nanoscience Group, School of Physics and Astronomy, University of Nottingham, Nottingham NG7 2RD, United Kingdom.
E-mail address: richard.woolley@physics.org (R.A.J. Woolley).
[1] Group web page: http://www.nottingham.ac.uk/physics/research/nano/.

0039-6028/$ - see front matter © 2007 Elsevier B.V. All rights reserved.
doi:10.1016/j.susc.2006.12.030

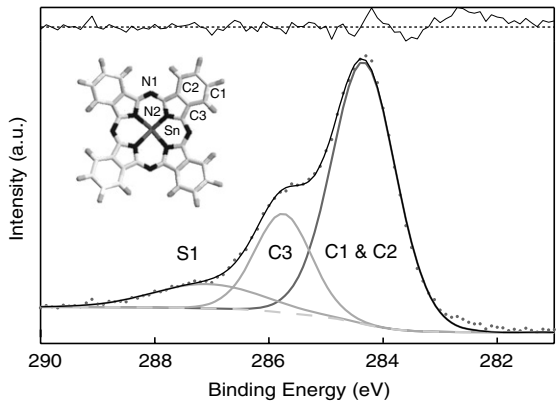

Fig. 1. C 1s XPS spectrum for a thick SnPc film. The fitting parameters are given in Table 1. Inset: The structure of tin phthalocyanine. Labels are defined in the text.

adsorbed on an atomically flat substrate the molecular axis lies parallel with the surface plane [5]. This can have a considerable impact on the efficiency of photovoltaic and other organic devices [6].

For these reasons, a number of groups have focussed on elucidating the interactions of phthalocyanine molecules with metal, semimetal, and semiconductor surfaces. SnPc has attracted attention due to its aplanar character and its adsorption on a variety of substrates including graphite [7], Au [7], Ag [8], and InSb [9] has thus been examined. Of particular importance to the present study, the SnPc/Ag(1 1 1) system has very recently been investigated with normal incidence X-ray standing wave spectroscopy (NIXSW) [10,11] by Stadler et al. [12] who found that the incommensurate lattice formed by annealing a multilayer film at a temperature of ~290 °C comprised molecules adsorbed in a Sn-down geometry. Importantly, a variety of coverage-dependent incommensurate superstructures have been observed in, as yet, unpublished SPA-LEED measurements for SnPc/Ag(1 1 1) [40]. The observation of this range of structures highlights the importance of intermolecular interactions (and the balance of intermolecular and molecule–substrate forces) in the SnPc/Ag(1 1 1) system.

Stadler et al.'s NIXSW investigation used photoelectron emission from the Sn 3d core-level as the probe of adsorption of the X-ray standing wavefield by the tin atom at the centre of the phthalocyanine molecule. As is now well-established [13], the extraction of structural parameters from NIXSW data can be complicated by a number of phenomena, depending on the signal used to monitor X-ray absorption. With photoelectron yield, the contribution of higher order (multipole) contributions beyond the standard dipole approximation must be taken into consideration [14]. This is, perhaps surprisingly, the case even for the relatively low photon energies typically used in XSW (a few keV). (As pointed out by Woodruff [15], the conventional view for quite some time was that non-dipole effects were significant only for much harder X-rays (>20 keV).) As discussed briefly below, the asymmetry in photoelectron emission arising from the higher order components of the electromagnetic field – in particular, the *cross terms* involving the electric quadrupole and magnetic dipole terms, $E1 \cdot E2$ and $E1 \cdot M1$ – can be formally taken into account using an asymmetry parameter, Q [14,16].

Auger electron emission does not suffer from the non-dipole asymmetry problem. One might then imagine that Auger-based NIXSW is rather better suited to the robust determination of accurate structural parameters. Unfortunately, however, for emission involving relatively shallow core-levels, Auger-based XSW is plagued by a different experimental artifact: the excitation of adsorbate Auger emission by inelastic and secondary electrons from the bulk crystal. The energy 'threshold' at which the dominant contribution to the adsorbate Auger signal becomes the excitation by the incident X-ray wavefield remains ill-defined. Although some authors suggest that the threshold energy should occur in the range 500–1000 eV [19,15], it is clear that further work on a diverse range of systems is required to clarify the importance of "bulk-excited" Auger contributions to the XSW signal. An interesting element of the study reported here is that for the Sn MNN Auger emission used to acquire our XSW data, the Sn M_4 binding energy is 498 eV, very close to the threshold suggested by some authors [19].

We note at this point that, for reasons described in the following section, it was not possible to apply the "ratioing" method previously put forward by Woicik et al. [17] to extract "pure" surface-related information from the total (i.e. bulk + surface) XSW signal. (Indeed, and as we shall discuss in a later paper [38], the Woicik et al. method is not generally well-suited to the extraction of quantitative structural parameters from XSW data.) Importantly, and notwithstanding the possible contribution of bulk-excited electrons to our Sn MNN spectra, we find that the structural parameters derived from our Auger XSW study largely agree within experimental error with those determined from XSW measurements of SnPc/Ag(1 1 1) based on Sn 3d photoemission signals [12]. An important exception is the observation of a rather higher coherent fraction for the $(\bar{1}\,1\,1)$ which we argue arises from a relatively small SnPc domain size.

2. Normal incidence X-ray standing wave spectroscopy

NIXSW is a powerful technique for the determination of adsorption sites [10,11,15,21] and has been used to study a variety of adsorbed molecules on a range of substrates. Using a single crystal substrate, backscattered X-rays will occur at the Bragg condition for normal incidence. The superposition of illuminating and reflected X-rays produces a standing wave field which has a periodicity in intensity equal to that of the scattering planes. Varying the incident photon energy within the reflectivity range moves the standing wave nodal and anti-nodal planes with respect to the crystal lattice. An atom 'bathed' in the wavefield will

emit photoelectrons, Auger electrons and/or X-ray photons with a yield, Y_p, given by [22]:

$$Y_p = 1 + R + 2\sqrt{R} f_{co} \cos(\phi - 2\pi D), \quad (1)$$

where

$$R = |E_H/E_0|^2 \quad (2)$$

is the reflectivity and E_0 and E_H are the incident and Bragg-reflected electric fields which produce the standing wave of phase ϕ. The terms which yield structural information are D, the coherent position (that is, the distance of the absorber site as a fraction of lattice spacing from the diffracting planes) and f_{co}, the coherent fraction, which is generally interpreted as the degree of order associated with site occupation.

With the X-ray energies used for NIXSW, non-dipole considerations are important when monitoring photoemission yields [14]. An asymmetry parameter, Q, is introduced to account for the difference between photoemission intensity from incident and reflected X-ray wavefields. A general formalism for the inclusion of multipole interference effects was developed by Vartanyants and Zegenhagen [16]. A simple method for determining Q is to compare the absorption yield and reflectivity for a thick, disordered multilayer film of an adsorbate, for which $f_{co} = 0$. In this case the absorption profile becomes

$$Y_p = 1 + \frac{1+Q}{1-Q} R. \quad (3)$$

As described in the introduction, Auger emission-derived XSW spectra (particularly involving low lying core-levels) can be contaminated with a bulk-excited signal. Methods for extracting this signal have been put forward by Woicik et al. [17], Shard and Cowie [18], Pacilé et al. [19], and Stanzel et al. [20]. The approach adopted by Stanzel et al. is certainly the most comprehensive and advanced but necessitates very good estimates of the angular distribution of photoelectron emission, the angular acceptance of the analyser (at the kinetic and pass energies of interest), the transmission properties of the analyser, and the contribution of electrons which strike the adsorbate layer at grazing incidence.

The 'ratio-ing' approach put forward by Woicik et al. [17] is simpler and is in principle system-independent. Although we initially attempted to use this method to extract the pure surface XSW signal from the total XSW spectrum, the ratioing technique is: (i) (as pointed out by Woicik et al. [17]) not very well-suited to XSW data involving adsorbates whose associated coherent position gives rise to a bulk-like XSW curve, as is the case for the SnPc/Ag(1 1 1) superstructure we study, and (ii) ill-suited to the extraction of accurate quantitative structural parameters for *any* adsorbate position. We shall return to a discussion of the Woicik et al. method – which is beyond the scope of this paper – in a future publication [38]. For now, we simply note that the Woicik et al. method cannot be applied to the extraction of the pure photon-induced XSW signal from our Sn MNN XSW spectra. The structural parameters derived from our study are, however, in good agreement with those determined by Stadler et al.'s Sn 3*d* photoemission XSW data [12], suggesting that for the Auger electron energies used in our study, electrons originating from the bulk Ag crystal do not strongly influence the results.

3. Experimental

Measurements were carried out on beamline 4.2 of the Synchrotron Radiation Source (SRS) at Daresbury, UK. Photoemission spectra were recorded using a hemispherical analyser (PSP [23]) with an acceptance angle of between 9° and 13° for the kinetic energies and pass energy (100 eV) used for our measurements. The analyser was positioned at 40° to the incoming light (provided by a double crystal (InSb) monochromator). The substrate, a Ag(1 1 1) single crystal, was cleaned in UHV using standard argon ion sputter and thermal annealing cycles of 550 °C. No contamination of the surface was detected using X-ray photo electron spectroscopy (XPS). (An unmonochromated Mg Kα source was used for all XPS measurements, unless otherwise stated, giving a FWHM of 1.2 eV for the Ag $3d_{5/2}$ linewidth.)

NIXSW spectra were obtained firstly by orienting the substrate such that at the Bragg energy the reflectivity was maximised. The subsequent standing wave spectra were obtained by incrementally increasing the photon energy through the reflectivity region. Adsorbate and substrate NIXSW spectra were recorded simultaneously with the latter giving a measure of the Bragg position and degree of instrumental broadening. The structural quality of the crystal was assessed using low energy electron diffraction (LEED) and NIXSW measurements of the substrate's Ag MNN and Ag 3d spectra. A sharp (1×1) LEED pattern with a low background was obtained, whilst the NIXSW structural parameters of $f_{co} = 0.84 \pm 0.09$ and $D = 0.98 \pm 0.02$ for the $\langle 1\,1\,1 \rangle$ reflection indicated that the mosaicity of the crystal was acceptable.

SnPc molecules 97% (Sigma Aldrich) were purified by vacuum sublimation cycles [24] before being introduced into the experimental chamber where they were then thoroughly degassed in a standard Knudsen cell up to and just beyond the deposition temperature of 410 °C (which was approximately 1 ML/min). In all evaporated films no contaminants were detected and the Sn 3d:C 1s core-level ratio was found to be 0.83 ± 0.02 ($h\nu$ = Mg Kα), which agrees with that expected from consideration of the theoretical photoemission cross sections and the stoichiometry of the molecule (C:N:Sn = 32:8:1).

4. Results and discussion

Films thick enough to mask detection of substrate photoemission were grown on the Ag(1 1 1) substrate while it was held at room temperature. This was to ensure

disordered growth, confirmed from the absence of any LEED pattern, suitable for calculating the various NIXSW asymmetry parameters required [25] for fitting the C 1s core-level XSW spectra. The Q value we determined from the C 1s XSW data for a disordered multilayer SnPc film was 0.22 ± 0.01, in very good agreement with that measured by Stadler et al. [12].

XPS measurements of the thick films gave "signature" phthalocyanine C 1s spectra, as shown in Fig. 1, consisting of, in order of intensity: (i) photoemission due to the C–C bonds in the 4 benzene rings, C_{1+2}; (ii) a second peak due to the C–N bond of the pyrrol carbons, C_3, and, (iii) a shake-up peak, S_1, arising from the $\pi \rightarrow \pi^*$ transition due to the pyrrol ionisation channel. A four component fit, to include a shake-up feature, S_2, due to the main C_{1+2} emission has been proposed by Niwa et al. [26]. This fourth component, and a possible fifth peak are the subject of considerable discussion in the literature [26–33]. Due to the rather poor resolution of our XPS measurements, we cannot justify a four component fit and have instead opted for a three component fit [28] using a Shirley background, Voigt functions for the two C_{1+2} and C_3 core level components, and a Gaussian function for the shake-up feature S_1 (the fitting parameters are given in Table 1).

Upon annealing, the SnPc multilayer was found to desorb around 300 °C, as was clear from a measurement of the ratio of the C 1s and Ag 3d peak intensities. Compared to the thick film, both C 1s and Sn 3d photoemission peaks shifted to lower binding energy by 0.3 eV. This shift towards lower binding energy has previously been observed in other phthalocyanine/metal systems [34] and has been proposed to arise from a subtle interplay of initial state (band bending in the thick organic film and interfacial interactions for the monolayer system) and final state effects. Again, our unmonochromised XPS measurements do not allow us to discuss these core-level shifts in detail. We note, however, the absence of new components in the Sn 3d spectrum for adsorbed, as compared to bulk, SnPc

Table 1
Best fit parameters for C 1s XPS spectra. An approximation to the analytical convolution of Gaussian and Lorenzian functions was used for fitting the core levels with weighting values of G(30):L(70)[a]

		BE (eV)	FWHM (eV)
Bulk	C_{1+2}	284.3	1.32
	C_3	285.7	1.17
	S_1	287.1	2.25
ML	C_{1+2}	284.0	1.38
	C_3	285.3	1.57
	S_1	287.0	2.22

[a] The approximation to the Voigt lineshape used in our fitting procedure is given by the product of a Gaussian and Lorentzian, $GL(x,F,E,m) = \frac{\exp((-4ln2)(1-m)\frac{(x-E)^2}{F^2})}{1+4m\frac{(x-E)^2}{F^2}}$ where x is the energy scale, E is the peak intensity, F is the width of both the Lorentzian and Gaussian line shapes, and $m = p/100$ such that p is the percentage of Lorentzian character; $p = 0$ defines a purely Gaussian lineshape. Further details are available at http://www.casaxps.com.

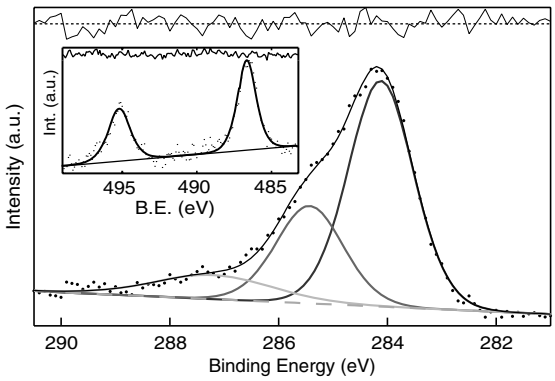

Fig. 2. C 1s spectrum for a 1 ML coverage of SnPc. Inset: Sn 3d spectrum of the same film.

(inset Fig. 2). A Sn(0)-related component has been observed [35] when SnPc undergoes a substitution reaction on an Fe surface. Our XPS data indicate that the Sn atom has not dissociated from the pthalocyanine molecule, in agreement with the arguments of Stadler et al. on the basis of their XSW results [12].

Although LEED patterns were obtained from SnPc monolayers prepared by annealing multilayer films at a temperature of ~300 °C, higher quality films, as indicated by significantly sharper LEED patterns (see Fig. 3), could be obtained by depositing SnPc onto a clean Ag(1 1 1) substrate held at the multilayer desorption temperature. A comparison of core-level peak intensities indicated that the SnPc coverage associated with the molecular assembly prepared in this manner was ~0.75 ML, where 1 ML is taken as the coverage associated with the film prepared by annealing a multilayer at 300 °C.[2] The line-shape of the Sn 3d spectrum was identical to that shown in the inset to Fig. 2. Due to the large size of the unit cell, low beam energies were required to produce good quality superstructure diffraction patterns meaning that the positions of the substrate and adsorbate spots could not be observed simultaneously. We therefore used a procedure similar to that outlined by Lackinger et al. [36], which is based on plotting the distance between adjacent spots vs. $1/\sqrt{E}$ (where E is the beam energy), to determine the *average* SnPc superstructure unit cell dimension. (As discussed below, the unit cell is not square.) This average value was 15.2 ± 0.4 Å. It is also important to note that neither of the basis vectors of the SnPc superstructure aligned with the Ag(1 1 1) surface basis vectors. The (incommensurate) SnPc supercell is orientationally misaligned (with respect to the Ag(1 1 1) surface) by $5 \pm 1°$.

We have used the LEEDPAT2 application [37] to determine the "best fit" to the experimental LEED pattern shown in Fig. 3. The LEEDPAT2-derived pattern is super-

[2] It is possible that annealing at this temperature produces a coverage somewhat below a nominal close-packed monolayer. Unfortunately, we did not have an STM capability on the beamline end-station and could not definitively determine the absolute molecular coverage.

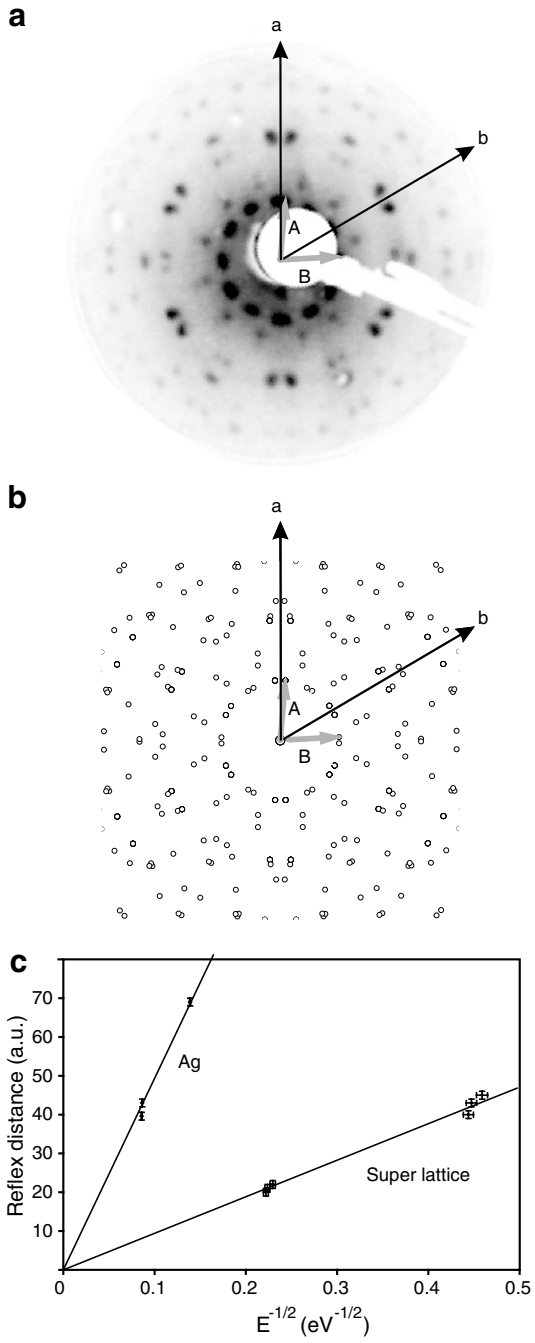

Fig. 3. (a) LEED pattern (beam energy: 20 eV) from a 0.75 ML coverage of SnPc on Ag(1 1 1). (b) A simulation of the pattern generated using LEEDPAT2. (c) Plot of various LEED spot distances for the super structure and substrate with corresponding beam energies (see text).

imposed on the experimental pattern and corresponds to an incommensurate lattice described approximately as following:

$$\begin{bmatrix}\mathbf{A}\\ \mathbf{B}\end{bmatrix} = \begin{bmatrix}5.01 & -0.53\\ 2.73 & 5.99\end{bmatrix}\begin{bmatrix}\mathbf{a}\\ \mathbf{b}\end{bmatrix}$$

where **A**, **B** are the basis vectors of the superstructure and **a**, **b** those of the underlying Ag(1 1 1) surface (see Fig. 4).

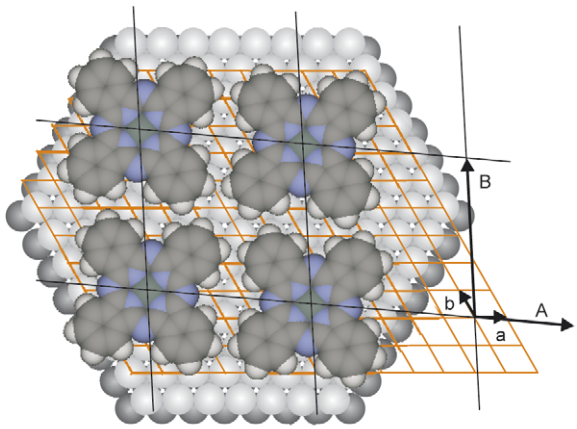

Fig. 4. The unit cell proposed for the SnPc/Ag(1 1 1) superstructure discussed in the text.

This superstructure is different from those previously studied by Stadler et al. [12], Lackinger [39], Lackinger and Hietschold [8], or Hansen [40]. (The SnPc system exhibits a rich variety of coverage-dependent structures [40].) The formation of incommensurate lattices usually involves a delicate balance of intermolecular and molecule-substrate interactions and it is thus not so surprising that variations in sample preparation (i.e. deposition on a hot substrate vs multilayer deposition with subsequent annealing) will yield markedly different superstructures for the SnPc/Ag(1 1 1) system. Moreover, there is a significant difference in coverage for the incommensurate structure investigated in this work and that studied by Stadler et al. [12].

The lengths of the basis vectors associated with the superstructure are $|\mathbf{A}| = 15.03$ Å and $|\mathbf{B}| = 15.31$ Å; it is not possible to reproduce key features of the LEED pattern if the lengths of the superstructure basis vectors are set equal. The angle between the superlattice vectors is 98° and the cell is rotationally displaced by 5° from the underlying Ag(1 1 1) surface lattice. Moreover there are six separate domains. Although it was generally difficult to resolve pairs of spots in the central ring of the LEED pattern (rather than blurred individual spots), this pairing of spots was indeed visible at certain beam energies (~23 eV).

As the SnPc superstructure is associated with an extremely dilute concentration of Sn atoms *and* the experiment was performed on a 2nd generation synchrotron source, very long integration times were required for the acquisition of the NIXSW spectra. The Sn MNN XSW spectra data in Fig. 7 were generated by integrating under the Sn MNN Auger emission (a typical spectrum is shown in Fig. 5) after subtraction of an appropriate background (also shown in the inset). The best fit parameters extracted from the Sn MNN XSW spectra (i.e. coherent position, D, and coherent fraction, f_{co}) for both the (1 1 1) and the ($\bar{1}$ 1 1) reflections are listed in Table 2. The structural parameters we have determined are very similar to those determined by Stadler et al. [12] for the incommensurate SnPc/Ag(1 1 1) system, albeit for a different superstructure.

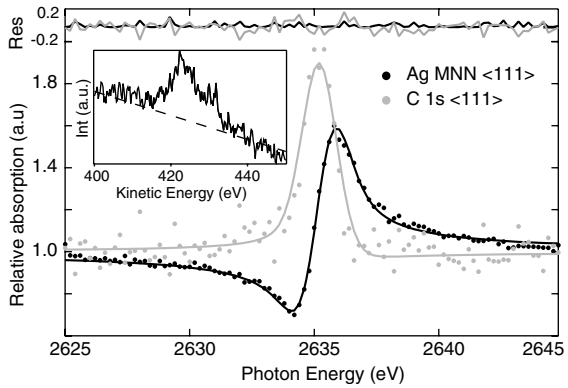

Fig. 5. NIXSW profiles derived from the substrate Ag MNN Auger emission and the C 1s photoemission signal. Inset: Sn MNN Auger spectrum.

Table 2
Structural parameters extracted from best fits to NIXSW data using dynamical theory

Structural parameters	$\langle 1\,1\,1\rangle$		$\langle \bar{1}\,1\,1\rangle$	
	D	f_{co}	D	f_{co}
Sn	0.98(4)	0.69(8)	0.90(5)	0.31(8)
C	0.53(7)	0.36(9)	0.48(7)	0.17(9)

Although XSW therefore appears not to be capable of differentiating directly between different incommensurate SnPc superstructures (in terms of the position of the central Sn atom), it is interesting to note that we see a clear difference in the coherent fraction for the $(\bar{1}\,1\,1)$ reflection as compared to the measurements of Stadler et al. [12].

Given that the SnPc superstructure is incommensurate, it might be initially expected that the coherent fraction associated with the $(\bar{1}\,1\,1)$ reflection would be very close to zero: an ideal incommensurate structure would comprise adsorbates in all possible registries across the substrate surface. La Rocca and Zegenhagen [41] have, however, shown that even an adsorbed 2D liquid can be associated with a coherent fraction significantly larger than zero. They make the important point that a correlation of the adsorbate positions with the substrate structure – due to the response of the adsorbate to the underlying periodic potential – will yield $f_{co} > 0$. Furthermore, for multi-domain systems, where the lateral extent of each incommensurate domain is constrained, remarkably high values (~0.4) of the coherent fraction have previously been observed [42].

As evidenced by the rather broad LEED spots arising from the SnPc superstructure (as compared to the widths of the spots arising from the Ag(1 1 1) surface), the domain size of the incommensurate SnPc superstructure is rather small. This low domain size narrows the distribution of Sn atom positions parallel to the Ag(1 1 1) surface (as compared to an "infinitely extended" incommensurate overlayer), giving rise to a larger-than-expected coherent fraction for the $(\bar{1}\,1\,1)$ reflection. Although, as shown in Table 2, we obtain values of the coherent fraction which are somewhat higher than those determined by Stadler et al. [12] for an incommensurate SnPc superstructure on Ag(1 1 1), it is not unexpected that variations in the sample preparation procedure could give rise to markedly different domain sizes and modify the response of the adsorbate to the periodic potential of the Ag(1 1 1) lattice. A detailed STM study of the effects of sample preparation conditions on SnPc superstructure formation on Ag(1 1 1) is required and is planned.

We now turn to the structural parameters extracted from the carbon-related XSW data. Due to difficulties associated with achieving a good signal-to-noise ratio when removing the background from C KVV spectra, the C 1s signal was used in NIXSW measurements (see Fig. 5). Positional information relating to carbon within the molecule will be associated with a low coherent fraction (due to the spread in positions of the carbon atoms). The coherent position, D, relates, however, to the *average* position (assuming that the associated coherent fraction is substantially greater than 0 and the coherent position is therefore well-defined). We take D to represent an overall position close to the centre of the planes of the benzene rings as these account for the majority of carbon atoms within the molecule. We find this average position to be 3.61 ± 0.16 Å from the (1 1 1) plane (see Fig. 6) with an associated coherent fraction of 0.36 ± 0.09. Although the C 1s coherent fraction we derive is within error of that reported by Stadler et al. [12], we find that the carbon atoms are, on average, located substantially further (by ~0.5 Å) from the Ag(1 1 1) surface plane for the SnPc superstruc-

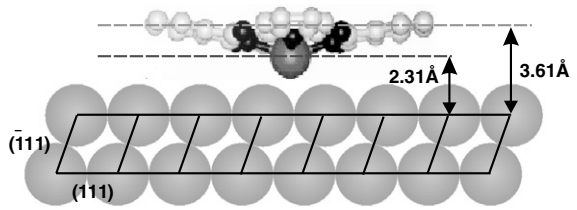

Fig. 6. Projected position of the SnPc molecule on the Ag(1 1 1) surface.

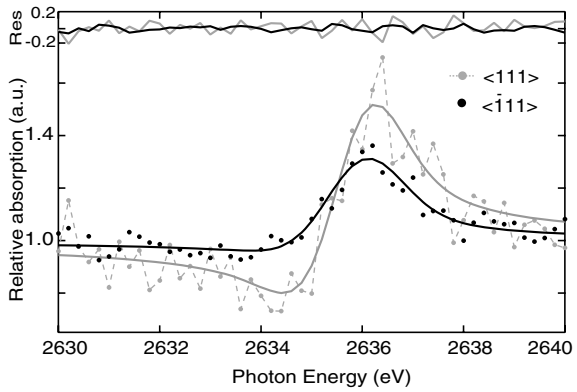

Fig. 7. NIXSW profiles for the Sn atom of SnPc measured using Sn MNN Auger emission.

ture prepared by deposition onto a hot substrate as compared to that formed by annealing a pre-deposited multilayer film. The Sn-to-C separation of ~1.3 Å is also somewhat larger than the 1.01 Å value observed for gas phase SnPc [43], suggesting a weaker interaction of the benzene rings of the SnPc molecule with the Ag(1 1 1) surface than was observed by Stadler et al. [12].

5. Conclusions

Deposition of tin phthalocyanine molecules onto an Ag(1 1 1) surface held at ~300 °C produces an incommensurate overlayer whose superstructure ($|\mathbf{A}| = 15.03$ Å, $|\mathbf{B}| = 15.31$ Å, $\alpha = 98°$) and, thus, unit cell size differ considerably from those produced by deposition of a thick SnPc overlayer with subsequent annealing [12]. This result by itself suggests that there is a wide parameter space associated with the synthesis of SnPc superstructures on the Ag(1 1 1) surface. Using Auger, rather than photoemission, detection for our XSW data acquisition we find that the coherent position and coherent fraction associated with the adsorbed SnPc molecules for the (1 1 1) substrate reflection are remarkably similar to those determined by Stadler et al. [12] for a different (but also incommensurate) unit cell. For the $(\bar{1}\,1\,1)$ reflection, however, we observe a coherent fraction value which is rather larger than expected for an incommensurate superstructure and which most likely arises from a correlation of the adsorbate positions with the underlying periodic potential of the substrate lattice and, as suggested by the broad LEED spots arising from the SnPc superstructure, a small domain size.

While the distance between the Sn atom and the Ag(1 1 1) surface is similar for both the incommensurate structure studied here and that investigated by Stadler et al. [12], differences in the bonding interactions are evident from the C 1s XSW spectra. Stadler et al. observe a significant bending of the molecule and shortening of the Sn to carbon distance whereas we find a bending in the opposite direction – *away* from the silver surface – with a Sn to carbon separation of ~1.3 Å.

Acknowledgements

We gratefully acknowledge both Markus Lackinger and Christoph Stadler for very helpful discussion and the provision of data prior to publication (including Refs. [39,40]). We thank Prof. Rob Jones, The University of Nottingham, for providing the *XSWFIT* IGOR macro that was used as a test bed for subsequent analysis programs and also for the substrate fitting parameters. Discussions with Bruce Cowie, Australian Synchrotron on the 'ratio-ing' method of XSW analysis have been invaluable. Similarly, we thank a referee of the original version of the manuscript for their very helpful and perceptive comments on the 'ratio-ing' analysis. Finally, we thank the Engineering and Physical Sciences Research Council (ESPRC) for funding and the Council for the Central Laboratories of the Research Councils (CCLRC) for the provision of beamtime at Daresbury SRS under award 41201.

References

[1] J.A. Theobald, N.S. Oxtoby, N.R. Champness, P.H. Beton, T.J.S. Dennis, Langmuir 21 (2005) 2038.
[2] C. Joachim, J.K. Gimzewski, A. Aviram, Nature 408 (2000) 541.
[3] C. Leznoff, A. Lever, Pthalocyanines: Propertise and Applications, John Wiley & Sons Inc., 1996.
[4] P.N. Day, Z.Q. Wang, R. Pachter, Theochem. J. Mol. Struct. 455 (1998) 33.
[5] M. Nakamura, Y. Morita, Y. Mori, A. Ishitani, H. Tokumoto, J. Vac. Sci. Technol. B 14 (1996) 1109.
[6] J.R. Ostrick, A. Dodabalapur, L. Torsi, A.J. Lovinger, E.W. Kwock, T.M. Miller, M. Galvin, M. Berggren, H.E. Katz, J. Appl. Phys. 81 (1997) 6804.
[7] K. Walzer, M. Hietschold, Surf. Sci. 471 (2001) 1.
[8] M. Lackinger, M. Hietschold, Surf. Sci. 520 (2002) L619.
[9] E. Salomon, T. Angot, N. Papageorgiou, J.M. Layet, Surf. Sci. 596 (2005) 74.
[10] D.P. Woodruff, D.L. Seymour, C.F. McConville, C.E. Riley, M.D. Crapper, N.P. Prince, Phys. Rev. Lett. 58 (1987) 1460.
[11] T. Ohta, H. Sekiyama, Y. Kitajima, H. Kuroda, T. Takahashi, S. Kikuta, Jpn. J. Appl. Phys. Lett. 24 (1985) L475.
[12] C. Stadler, S. Hansen, F. Pollinger, C. Kumpf, E. Umbach, T.-L. Lee, J. Zegenhagen, Phys. Rev. B 74 (2006) 035404.
[13] D.P. Woodruff, Rep. Prog. Phys. 68 (2005) 743.
[14] C.J. Fisher, R. Ithin, R.G. Jones, G.J. Jackson, D.P. Woodruff, B.C.C. Cowie, J. Phys. Condes. Matter 10 (1998) L623.
[15] M. Yu, D.P. Woodruff, N. Bovet, C.J. Satterley, K. Lovelock, R.G. Jones, V. Dhanak, J. Phys. Chem. B 110 (2006) 2164.
[16] I.A. Vartanyants, J. Zegenhagen, Solid State Commun. 113 (1999) 299.
[17] J.C. Woicik, T. Kendelewicz, K.E. Miyano, P.L. Cowan, C.E. Bouldin, B.A. Karlin, P. Pianetta, W.E. Spicer, Phys. Rev. Lett. 68 (1992) 341.
[18] A.G. Shard, B.C.C. Cowie, J. Phys. Condes. Matter 10 (1998) L69.
[19] D. Pacile, M. Papagno, A. Cupolillo, G. Chiarello, L. Papagno, J. Electron Spect. Relat. Phenom. 135 (2004) 201.
[20] J. Stanzel, W. Weigand, L. Kilian, H.L. Meyerheim, C. Kumpf, E. Umbach, Surf. Sci. 571 (2004) L311.
[21] J. Zegenhagen, Surf. Sci. Rep. 18 (1993) 199.
[22] D.P. Woodruff, Prog. Surf. Sci. 57 (1998) 1.
[23] http://www.pspvacuum.com/.
[24] S.R. Forrest, Chem. Rev. 97 (1997) 1793.
[25] F. Schreiber, K.A. Ritley, I.A. Vartanyants, H. Dosch, J. Zegenhagen, B.C.C. Cowie, Surf. Sci. 486 (2001) L519.
[26] Y. Niwa, H. Kobayash, T. Tsuchiya, J. Chem. Phys. 60 (1974) 799.
[27] L. Zhang, H. Peisert, I. Biswas, M. Knupfer, D. Batchelor, T. Chasse, Surf. Sci. 596 (2005) 98.
[28] L. Ottaviano, S. DiNardo, L. Lozzi, M. Passacantando, P. Picozzi, S. Santucci, Surf. Rev. Lett. 4 (1997) 59.
[29] S. Kera, M.B. Casu, K.R. Bauchspiess, D. Batchelor, T. Schmidt, E. Umbach, Surf. Sci. 600 (2006) 1077.
[30] H. Peisert, M. Knupfer, J. Fink, Surf. Sci. 515 (2002) 491.
[31] K.T. Park, A. Miller, K. Klier, R.L. Opila, J.E. Rowe, Surf. Sci. 529 (2003) L285.
[32] G. Dufour, C. Poncey, F. Rochet, H. Roulet, M. Sacchi, M. Desantis, M. Decrescenzi, Surf. Sci. 319 (1994) 251.
[33] N. Papageorgiou, Y. Ferro, E. Salomon, A. Allouche, J.M. Layet, L. Giovanelli, G. Le Lay, Phys. Rev. B 68 (2003) 235105.
[34] T. Schwieger, H. Peisert, M. Knupfer, Chem. Phys. Lett. 384 (2004) 197.
[35] J.W. Wells, G. Cabailh, D.A. Evans, S. Evans, A. Bushell, A.R. Vearey-Roberts, J. Electron Spect. Relat. Phenom. 141 (2004) 67.

[36] M. Lackinger, S. Griessl, W.M. Heckl, M. Hietschold, J. Phys. Chem. B 106 (2002) 4482.
[37] K. Hermann, M.A. Von Hove, <http://w3.rz-berlin.mpg.de/~hermann/LEEDpat/>.
[38] RAJ Woolley, KHG Schulte, MA Phillips, L. Wang, G. Miller, V.R. Dhanak, and P. Moriarty, unpublished.
[39] M. Lackinger, Ph.D. Thesis, Technische Universität Chemnitz, 2003.
[40] S. Hansen, Master's Thesis, Universität Wurzbürg, 2005.
[41] G.C. La Rocca, J. Zegenhagen, Phys. Rev. B 44 (1991) 13666.
[42] J. Zegenhagen, E. Fontes, Phys. Rev. B 45 (1992) 13721.
[43] C.Y. Ruan, V. Mastryukov, M. Fink, J. Chem. Phys. 111 (1999) 3035.